

ORIGINAL RESEARCH

Assessment of Machine Learning Models in Liquefaction Prediction with Emphasis on ROC Curve and AUC Index Differences

Agha kasiri Sh.^{1*} Shahraki M.² Agha kasiri S.³

Abstract:

This study presents a novel approach for predicting soil liquefaction potential, a critical concern in geotechnical engineering. Liquefaction refers to the behavior of soil under dynamic loading or transient shear wave excitation, during which the soil completely loses its shear strength and temporarily transforms into a fluid-like state. By integrating empirical geotechnical relationships with advanced machine learning techniques, the research offers a modern perspective on evaluating the likelihood of liquefaction occurrence. The analysis is based on data derived from Cone Penetration Test (CPT) records. Three soft computing models were implemented: Artificial Neural Networks (ANN), Logistic Regression (LR), and Neuro-Fuzzy Network. Their performance was evaluated using Receiver Operating Characteristic (ROC) curves. Among the models compared, Logistic Regression demonstrated superior performance, with the Area Under the Curve (AUC) from the “All” dataset reaching approximately 0.975, indicating high reliability in classification accuracy. In this study, the logistic regression model achieved an AUC of 0.975 on the full dataset, followed by the artificial neural network (AUC = 0.925) and the fuzzy logic system (AUC = 0.71).

Keywords:

Soil liquefaction potential, Artificial Neural Network, Logistic Regression, Neuro-Fuzzy Network, Cone Penetration Test (CPT)

*Corresponding author Email: Sh.aghakasiri@aiu.ir

1. Department of Civil Engineering, ST.C., Islamic Azad University, Tehran, Iran.

2. Department of Civil Engineering, Zah.C., Islamic Azad University, Zahedan, Iran. Email: Mehdi.shahraki@iau.ac.ir

3. Department of Civil Engineering, Babol Noshirvani University of Technology (NIT), Babol, Iran.

Email: sanazaghakasiry@gmail.com

1. Introduction

Liquefaction is one of the most critical phenomena influencing the instability of buildings and infrastructure during earthquakes, making it a key focus in seismic research and foundation design. Nearly every major earthquake results in widespread ground deformations due to soil liquefaction, leading to significant and often catastrophic damage to both soils and foundations. The characteristics of liquefaction can vary depending on geometry, soil type, and local conditions, influenced by several factors including unusual wave propagation, seismic amplification, and geological conditions such as grain distribution, soil density, and groundwater level [1].

Liquefaction is classified as a form of ground failure typically triggered by strong ground shaking during earthquakes. The first widely documented cases of severe liquefaction damage occurred during the 1964 Niigata earthquake in Japan and the 1964 Alaska earthquake in the United States [2]. Earthquakes have consistently attracted the attention of civil and geotechnical engineers, especially due to their role in triggering liquefaction [3]. Numerous researchers have studied the seismic behavior of soils and structures over the past decades [4-6].

Following the extensive liquefaction events observed in the 1964 Niigata and Alaska earthquakes, geotechnical researchers increasingly focused on understanding this phenomenon [7]. In Iran, liquefaction zonation studies commenced after the destructive Manjil earthquake, led by the International Institute of Earthquake Engineering and Seismology. The outcome was a national-scale liquefaction hazard map at 1:1,000,000 scale [8].

Over the past four decades, significant progress has been made in understanding the mechanisms and influencing factors of soil liquefaction. Initially, most research focused on clean sands, as it was believed that liquefaction occurred only in such soils and

that coarse- or fine-grained soils lacked the capacity to generate excess pore water pressure, which is the main cause of liquefaction. However, with the occurrence of recent earthquakes and observations of liquefaction in a wider variety of soils, researchers have expanded their studies to identify the influencing factors in both fine- and coarse-grained soils [9].

Ahmad et al. (2021) evaluated the performance of four machine learning (ML) algorithms for earthquake-induced liquefaction assessment using cone penetration test (CPT) data and field case histories [10]. García et al. (2011) developed a large database combining CPT, SPT, and Vs measurements with historical earthquake liquefaction performance records. They applied: (1) an artificial neural network (ANN) to map key index features to resistance parameters, (2) a fuzzy neural system for estimating liquefaction occurrence and developing a multidimensional fuzzy liquefaction index, and (3) a regression tree for generating or supplementing seismic loading information [11].

In a 2024 study, Liu et al. developed machine learning models to estimate building settlements induced by liquefaction. Five ML models ridge regression, partial least squares regression, random forest, gradient boosting decision tree, and support vector regression were trained on a database generated through numerical simulations involving various building soil profiles subjected to ground motions of different intensity measures [12]. Abbasimaedeh (2024) investigated liquefaction potential in seismic events using leading predictive models based on machine learning techniques such as logistic regression, decision trees, and support vector machines [13].

Ozsagir et al. (2022) evaluated machine learning approaches for predicting liquefaction potential in fine-grained soils using seven ML algorithms, including logistic

regression, artificial neural networks, decision trees, support vector machines, k-nearest neighbors, stochastic gradient descent, and random forest [14]. Obaidullah (2024) also applied four ML models logistic regression, support vector machine, decision tree, and Artificial Neural Networks to field-based liquefaction prediction, finding decision trees to be the most effective algorithm [15].

Kumar et al. (2021) proposed the application of deep learning algorithms for the assessment of soil liquefaction using Cone Penetration Test (CPT) data [16]. In a similar line of research, Raja et al. (2024) developed intelligent prediction models for lateral spreading caused by liquefaction, utilizing techniques such as Genetic Algorithms (GA), Artificial Neural Networks (ANN), and k-Nearest Neighbors (KNN) [17]. Mohammadi Kish et al. (2023) applied a fuzzy-incomplete clustering approach for liquefaction evaluation based on CPT and shear wave velocity (Vs) measurements [18]. More recently, Şehmusoğlu et al. (2025) implemented various artificial intelligence methods such as logistic regression and support vector machines for liquefaction prediction. Their findings highlighted the potential of machine learning tools in mitigating seismic risks associated with liquefiable soils [19].

In light of the increasing demand for reliable and rapid prediction of liquefaction potential, especially in urban areas prone to seismic activity, this study aims to evaluate and compare the performance of three soft computing models—Artificial Neural Networks (ANN), Logistic Regression (LR), and Neuro-Fuzzy systems. The integration of CPT-based data and advanced classification techniques aims to provide a robust framework for identifying liquefiable soils, contributing to safer geotechnical designs and informed urban planning. The structure of the paper is organized as follows: Section 3 presents CPT testing fundamentals, Section 4 discusses liquefaction hazard calculations, Section 4 elaborates on ML-based modeling approaches, and Sections 5–7 present model evaluation and performance analysis.

2. Literature Review

Numerous studies have been conducted to assess the effectiveness of machine learning techniques in predicting soil liquefaction. For example, Ahmad et al. (2021) applied multiple ML algorithms using CPT data and found that decision tree models had relatively high accuracy[10]. Ozsagir et al. (2022) implemented seven ML models for fine-grained soils, among which LR and ANN showed promising results[14]. Liu et al. (2024) focused on liquefaction-induced building settlement prediction using gradient boosting and random forest models[12]. In another study, Obaidullah (2024) concluded that decision trees outperformed SVMs and logistic regression in field-based prediction[15]. These comparative insights establish the foundation for this study and highlight the significance of model evaluation using ROC and AUC indices.

3. Cone Penetration Testing (CPT)

Since its introduction in geotechnical engineering, the Cone Penetration Test (CPT) has been widely employed in numerous applications such as bearing capacity estimation, shallow and deep foundation design, and liquefaction resistance assessment [20–24]. CPT allows for the efficient estimation of key soil parameters. In this context, Marzouk et al. (2024) provided a detailed review of the Standard Penetration Test (SPT) and its integration with deep learning techniques in civil engineering projects[25].

4. Calculation of Liquefaction Hazard

Determining the liquefaction resistance of soil based on analysis results requires the calculation or estimation of two variables. The first parameter is the Cyclic Stress Ratio (CSR), which indicates the level of cyclic loading that may be caused by an earthquake, and the second parameter is the Cyclic Resistance Ratio (CRR), which indicates the

soil's resistance to liquefaction. The cyclic stress ratio induced during an earthquake (CSR) is defined by Seed and Idriss (1971) as follows [26]:

$$CSR = 0.65 * (a_{max} / g) * (\sigma_v / \sigma'_v) * rd \quad (1)$$

where a_{max} is the peak horizontal ground acceleration during the earthquake, g is the gravitational acceleration, σ_v and σ'_v are the total and effective vertical stresses, respectively, and rd is the stress reduction coefficient. Average values for rd based on depth are defined by Liao and Whitman (1986) for engineering applications [27]:

$$rd = [1.0 - 0.00765z, \text{ for } z \leq 9.15m] \\ 1.174 - 0.0267z, \text{ for } 9.15 < z \leq 23m] \quad (2)$$

z is the depth (in meters). The Cyclic Resistance Ratio (CRR) is also defined by Robertson and Ride (1998) [28] as follows. In this method, it is necessary to adjust the cone tip resistance corrected for overburden stress ($qc1N$) when determining liquefaction resistance. The parameter $qc1N$ is normalized using the overburden stress correction factor (CQ) as shown in the equations below:

$$qc1N = CN * (qc / Pa) * (Pa / \sigma'_v)^n \quad (3)$$

$$CQ = (\sigma_v / \sigma'_v)^n \quad (4)$$

where qc is the measured cone tip resistance, CQ is the overburden stress correction factor, Pa is the reference pressure (e.g., $Pa = 100$ kPa if qc is in kPa or $Pa = 0.1$ MPa if qc is in MPa), and n is a coefficient that varies with soil type and is usually 0.5. The maximum value of $CQ = 2$ generally applies to shallow CPT data. The normalized cone resistance $qc1N$ is dimensionless.

Robertson and Wride (1998) indicated [28] that the CPT friction ratio increases with increasing fines content and soil plasticity. The granular characteristics of sandy soils can be directly estimated from CPT data using soil behavior type charts, such as the one shown in Figure 1 (Robertson, 1990) [29]. Also, the Soil Behavior Type Index (Ic) can be defined as follows [29]:

$$Ic = \sqrt{[(3.47 - \log Q)^2 + (\log F + 1.22)^2]} \quad (5)$$

$$Q = (qc1N / Pa) \quad (6)$$

$$F = (f_s / (qc - \sigma_v)) * 100\% \quad (7)$$

where Q is the normalized tip resistance, F is the normalized friction ratio, n is typically 1.0, and σ_v and σ'_v are the total and effective overburden stresses, respectively.

The boundaries of soil behavior type based on the Ic index are shown in Table 1.

Table 1: Soil Behavior Type Boundaries [29]

Classification	SBT (Figure 1)
Gravelly to Dense Sand	7
Sand: Clean Sand to Silty Sand	6
Sand Mixtures: Silty Sand to Sandy Silt	5
Silt Mixtures: Clayey Silt to Silty Clay	4
Clay: Silty Clay to Clay	3
Organic Soils	2

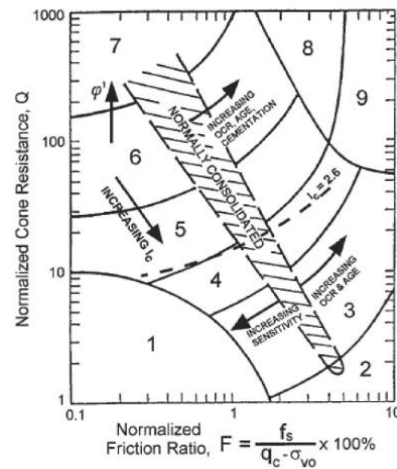


Fig. 1. Normalized CPT soil behavior type diagram, as proposed by Robertson in 1990[29].

The proposed equation to obtain the equivalent clean-sand normalized CPT resistance $qc1N_{Cs}$ as a function of measured resistance, soil characteristics, is as follows:

$$qc1N_{Cs} = qc1N * K_c \quad (8)$$

Here, K_c is the correction factor representing the soil's grain structure, defined by equations 9 and 10:

$$\text{If } Ic \leq 1.64, \text{ then } K_c = 1.0 \quad (9)$$

$$\text{If } Ic > 1.64, \text{ then } K_c = 5.581 * Ic^3 - 0.403 * Ic^4 - 21.63 \quad (10)$$

If $I_c > 2.6$, data should be directly plotted on Robertson's chart assuming $qc1N_{cs} = Q$. If $I_c \leq 2.6$, the power for Q calculation should be adjusted to $n = 0.5$ (i.e., calculate $qc1N$ using Eq. (3)), then recalculate I_c based on $qc1N$ and F. If the recalculated I_c remains below 2.6, the data should be plotted on the Robertson chart using ($n=0.5$). However, if the recalculated I_c fluctuates around 2.6, a value of ($n=0.75$) should be used for calculating $qc1N_{cs}$. Equations 5, 8, 9, and 10 can be combined to directly estimate the clean-sand equivalent normalized cone resistance $qc1N_{cs}$ from CPT data. Then, CRR for an earthquake magnitude ($M=7.5$) can be estimated using the simplified equations below:

$$\text{If } 50 \leq qc1N_{cs} < 160, \text{CRR} = 93 + 0.08 * qc1N_{cs} \quad (11)$$

$$\text{If } qc1N_{cs} < 50, \text{CRR} = 0.833 * qc1N_{cs} / 100 \quad (12)$$

5. Subsurface Layer Identification Using CPT and Deep Learning Techniques

Developing a model to describe the type, extent, and geotechnical properties of subsurface soil layers remains a fundamental task in geotechnical investigations. Traditionally, this modeling has relied on interpretations of field exploration data, such as trenches and boreholes, often constrained by the minimum number of tests required by relevant standards [30]. This process demands both broad expertise in subsurface data interpretation and region-specific knowledge. In many cases, such interpretations are supported only partially by empirical tools such as the Soil Behavior Type (SBT) charts proposed by Robertson or by analytical correlations [31-34]. Consequently, CPT-based interpretation for machine learning modeling often depends on the subjective judgment of engineers.

In recent years, numerous machine learning techniques have been proposed to address various geotechnical problems, including liquefaction assessment [22], pile settlement

prediction [21], and tunnel boring performance forecasting [35].

6. Selection of Data and Machine Learning Methods

6.1. Data Selection

The computational dataset employed in this study was primarily derived from field data obtained through Cone Penetration Tests (CPT) conducted in coastal cities of Mazandaran Province. In addition, supplementary datasets were extracted from previously published and peer-reviewed scientific literature to enhance the comprehensiveness and diversity of the training data [36,37].

6.2. Artificial Neural Network (ANN)

Artificial Neural Networks (ANNs) are among the most widely used machine learning techniques due to their ability to model complex, nonlinear relationships in data. Inspired by the structure and function of the human brain, an ANN is composed of numerous interconnected processing elements known as neurons. Each neuron receives signals from the input layer, processes them using an activation function, and transmits the result to the next layer via weighted connections.

These connections carry different weights that determine the importance of each input. The input signals are multiplied by these weights and summed together along with a bias term, then passed through activation functions in hidden layers. This flow of information from the input layer through hidden layers to the output layer is referred to as forward propagation. Conversely, during training, errors are propagated back from the output to adjust the weights this process is known as backpropagation.

ANNs can learn from large volumes of data and adapt their structure iteratively to minimize prediction errors, thereby improving their accuracy over time. Depending on the

nature of the problem, different activation functions may be applied. Once trained, the ANN can reliably classify or predict unseen data related to soil liquefaction [38].

6.3. Logistic Regression Method

Logistic regression is a supervised learning algorithm and a statistical model commonly used to estimate the probability of a binary outcome such as liquefiable vs. nonliquefiable conditions based on one or more independent input variables.

The model uses a logistic (sigmoid) function to map linear combinations of the input features into probabilities between 0 and 1. The logistic function is expressed as:

$$P = \frac{1}{1 + e^{-z}} \quad (13)$$

where z is a linear combination of input variables, bias, and coefficients.

$$z = \beta_0 + \beta_1 x_1 + \beta_2 x_2 + \dots + \beta_n x_n \quad (14)$$

The output value e represents the probability of a positive class (e.g., liquefiable soil). To optimize prediction performance, the algorithm adjusts feature weights by minimizing a cost function that measures the difference between predicted and actual outcomes. The logistic regression cost function is given by:

$$J(h, y) = -y \log(h) - (1 - y) \log(1 - h) \quad (15)$$

where y is the actual label, h is the predicted probability, and \log is the natural logarithm. Weight optimization is typically performed using gradient descent, and training continues until the cost function reaches its minimum.

Once trained, the model can be used to estimate the liquefaction potential of new data. Model performance is evaluated using metrics such as accuracy, precision, recall, and the Area Under the ROC Curve (AUC-

ROC). Overall, logistic regression offers a reliable and interpretable machine learning approach for assessing soil liquefaction potential, particularly when dealing with large datasets and complex variable interactions.

6.4. Fuzzy Logic System

Fuzzy logic provides a structured framework for handling uncertainty and imprecision in probabilistic systems. It is particularly effective in managing input-related uncertainties within datasets. A fuzzy inference system (FIS) consists of three core components: fuzzifier, inference engine, and defuzzifier. In fuzzy logic, each input variable is associated with a membership function, which graphically represents the degree of belonging of a variable to a fuzzy set. Based on expert judgment and data analysis, parameters such as the number, shape, and range of membership functions can be defined. The fuzzifier converts crisp inputs into fuzzy values, which are then processed by the inference engine using a set of predefined rules. The output is finally translated into a crisp value through the defuzzification process. Common types of FIS include: (1) Mamdani-type, (2) Sugeno-type, and (3) Tsukamoto-type fuzzy systems [39].

7. Data Analysis

Before calculating the Liquefaction Potential Index (LPI) in detail, a two-stage methodological approach is recommended. Initially, in a preliminary assessment, theoretical indicators based on geological, geomorphological, and hydrological data can be used to identify liquefaction-susceptible zones. Subsequently, Cone Penetration Test (CPT) data can be used to assess liquefaction resistance as a function of depth. In this study, a dataset containing seven input features was selected for use in different neural network models: earthquake magnitude, total stress, effective stress, peak ground acceleration, cone resistance, average shear stress, and

mean grain size (D50). The output variable was binary, representing whether a soil profile was susceptible to liquefaction or not.

8. ROC Curve Analysis

A gradient descent algorithm was used to iteratively update model weights until the cost function was minimized. Once trained, the model was applied to unseen data to predict liquefaction potential. Performance was assessed using accuracy, precision, recall, and area under the ROC curve (AUC-ROC). Among various models tested, logistic regression emerged as a reliable and effective method for evaluating liquefaction potential, capable of managing large datasets and modeling complex variable relationships.

results were visualized using Receiver Operating Characteristic (ROC) curves. The

AUC value, ranging from 0 to 1, reflects the discriminative power of the model—values closer to 1 indicate better performance. ROC curves plot sensitivity versus false positive rate, where a diagonal line indicates 50% random prediction accuracy. Generally, AUC values greater than 0.7 are considered acceptable for model validation purposes. In this study, the logistic regression model achieved an AUC of 0.975 on the full dataset, followed by the artificial neural network (AUC = 0.925) and the fuzzy logic system (AUC = 0.71). a comparative illustration of the ROC curves under the "ALL" dataset condition is presented in Fig.2 and a summary of the performance metrics for the evaluated models, including accuracy, precision, recall and AUC is presented in table 2.

Table 2: Model Performance Summary Table

Model	Accuracy	Precision	Recall	AUC
Logistic Regression	95.2%	93.5%	96.0%	0.975
Artificial Neural Network	91.8%	90.1%	93.2%	0.925
Fuzzy Logic System	81.5%	79.8%	82.6%	0.710

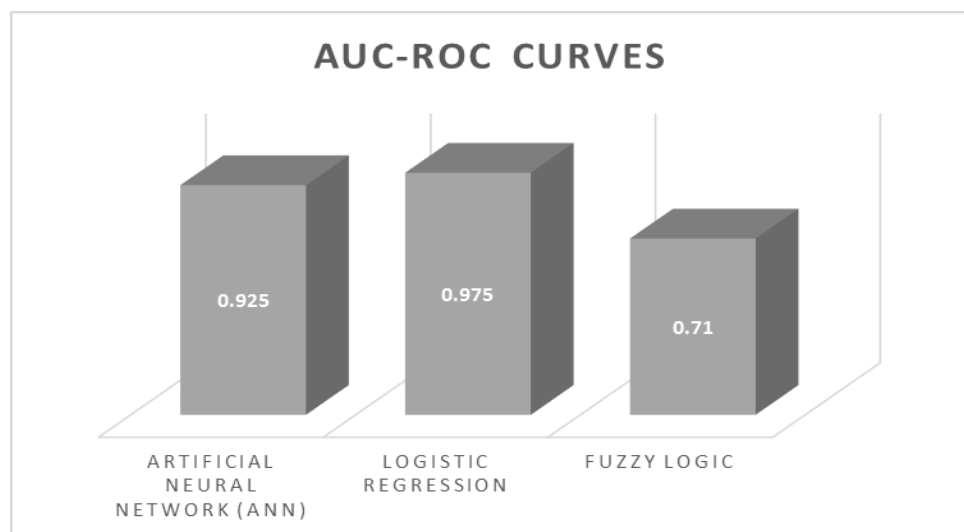


Fig. 2. The figure illustrates a comparative analysis of the ROC curves obtained from various models, based on the complete ('All') dataset

These results suggest that all models performed adequately, with logistic regression being the most accurate. ROC curves for

training, testing, and all-data scenarios across the three models (Artificial Neural Network

(ANN), logistic regression, and fuzzy logic) are shown in Figures 3-11.

The prediction of soil liquefaction plays a crucial role in seismic hazard analysis. To evaluate the effectiveness of each model in predicting LPI, ROC curve analyses were

performed in TRAIN, TEST, and ALL configurations, with results visualized in the corresponding figures.

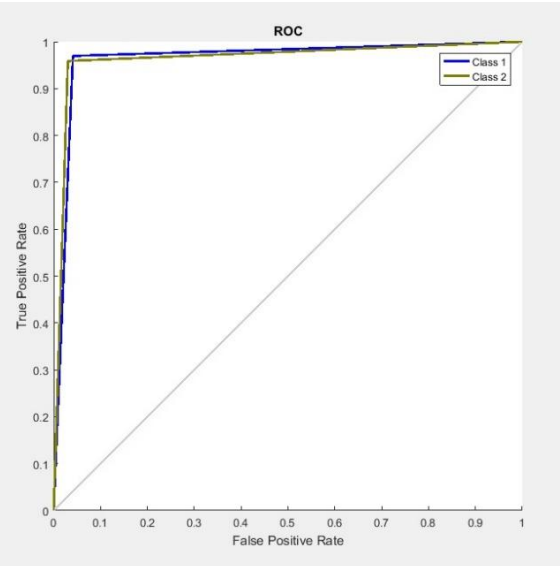


Fig. 3. The ROC curve corresponding to the train data in the artificial neural network.

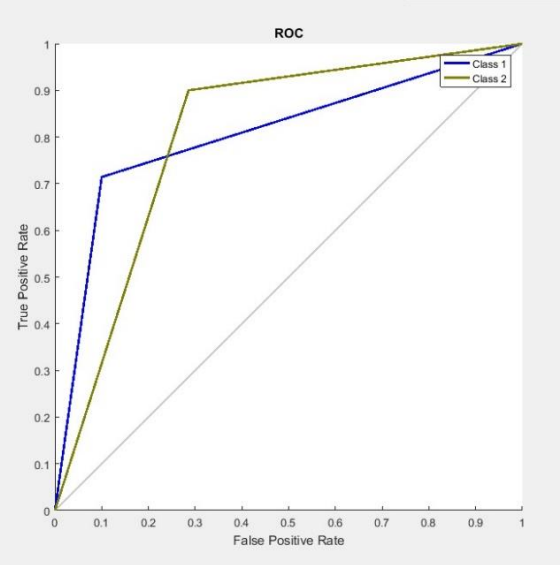


Fig. 4. The ROC curve corresponding to the test data in the artificial neural network.

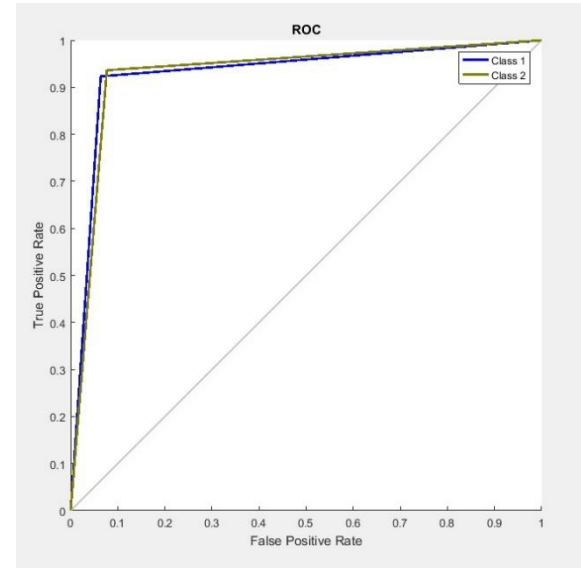


Fig. 5. The ROC curve corresponding to the ALL data in the artificial neural network.

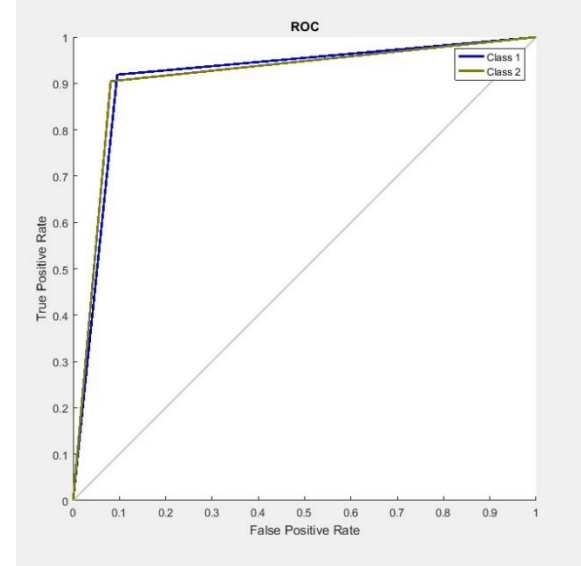


Fig. 6. The ROC curve corresponding to the train data in the Logistic Regression Method

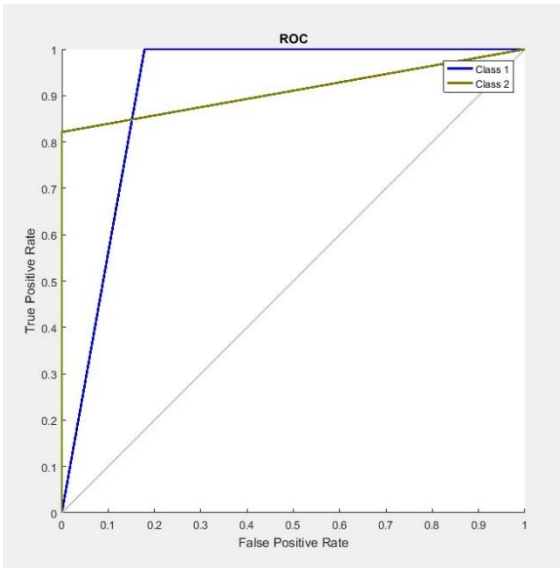


Fig. 7. The ROC curve corresponding to the test data in the Logistic Regression Method

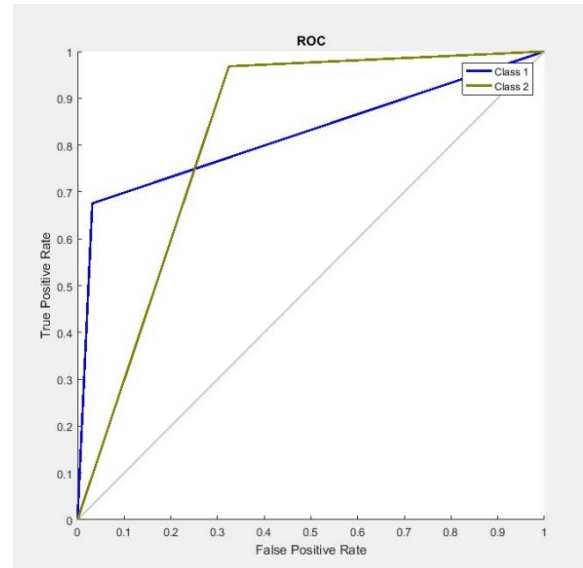


Fig. 9. The ROC curve corresponding to the train data in the Logistic Regression Method

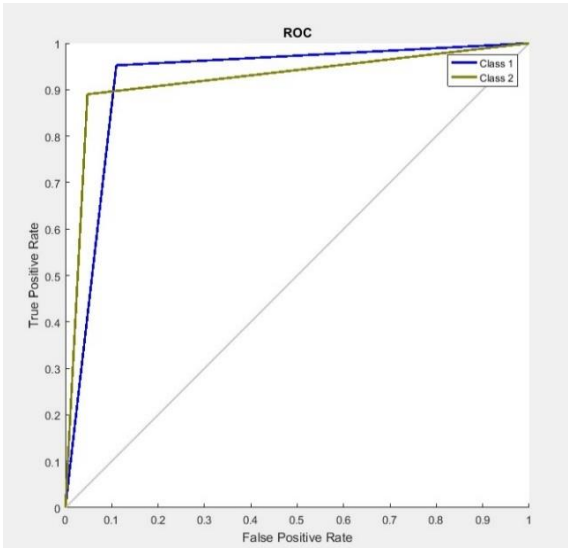


Fig. 8. The ROC curve corresponding to the ALL data in the Logistic Regression Method

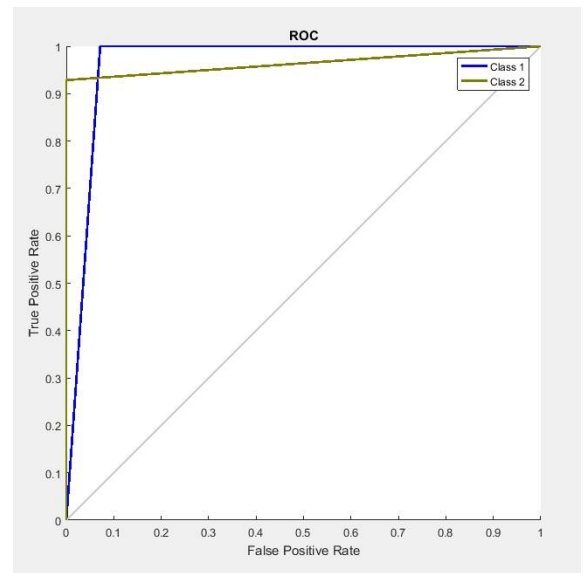


Fig. 10. The ROC curve corresponding to the test data in the Logistic Regression Method

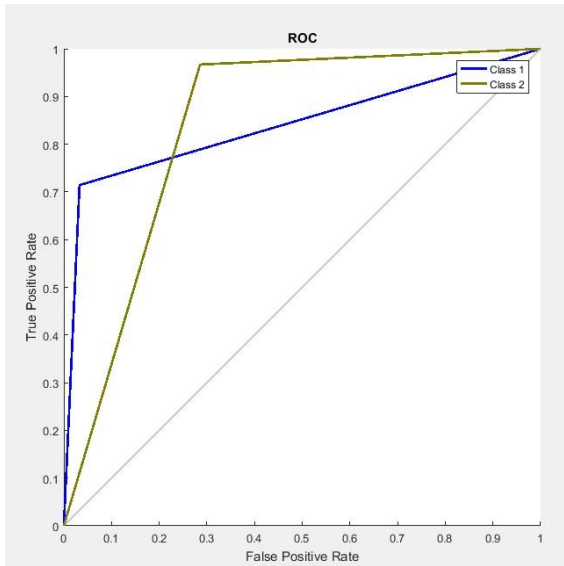


Fig. 11. The ROC curve corresponding to the ALL data in the Logistic Regression Method

9. Discussion

The results suggest that Logistic Regression (LR) outperforms both ANN and Fuzzy Logic in terms of classification metrics. This may be attributed to LR's capability in handling linear decision boundaries with a lower risk of overfitting. While ANN demonstrated strong predictive power, it may have been sensitive to parameter tuning and data imbalance. Fuzzy Logic, although interpretable, showed lower precision and recall, possibly due to simplified rule-based approximations. Comparing these findings with prior literature reinforces the reliability of LR for binary geotechnical classification tasks.

10. Conclusion

During liquefaction, soil loses its strength and behaves like a fluid under seismic loading, posing a significant threat to infrastructure and human life. Traditionally, engineers have relied on complex theoretical frameworks or empirical methods to assess liquefaction potential. However, these conventional approaches can be time-consuming, require extensive datasets, and may not fully capture the complex interactions among the influencing factors.

Deep learning offers a powerful alternative for predicting soil liquefaction. These algorithms can be trained on large datasets that include geotechnical parameters, seismic inputs, and historical liquefaction occurrences. In this study, MATLAB (version 2016a) was used to develop predictive models for liquefiable and non-liquefiable soil conditions through machine learning-based coding. Accuracy, precision, F1-measure, and recall were computed for three classification scenarios: liquefied, non-liquefied, and overall using an 80/20 train-test data split.

Given that the Cone Penetration Test (CPT) provides continuous subsurface data, it plays a key role in accurately identifying potentially liquefiable soil layers. Three ensemble learning-based machine learning models were developed to assess liquefaction potential, with emphasis placed on their performance during both the training and testing phases, as well as in the overall dataset.

Engineers and researchers can evaluate and compare model performance in predicting liquefaction sensitivity by considering the ROC-AUC metric. As shown in Figures 3 to 11, the Area Under the Curve (AUC) provides a quantitative measure of each classifier's performance. A higher AUC value indicates better model performance, where an AUC of 1.0 represents a perfect classifier. The ROC-AUC metric was chosen for this study as it enables comparison across various classification thresholds, making it particularly valuable in geotechnical applications where accurately identifying both liquefied and non-liquefied states is essential.

Among the evaluated models, the logistic regression classifier exhibited superior ROC curve performance compared to the artificial neural network (ANN) and fuzzy logic models.

In conclusion, among the models evaluated, Logistic Regression proved to be the most accurate and stable method for liquefaction prediction using CPT data. The study emphasizes the practicality of integrating

machine learning models in seismic hazard analysis. For future research, it is recommended to explore hybrid models, such as ensemble learning or deep CNN architectures. From a practical standpoint, local governments and urban planners can incorporate these predictive tools into early-warning systems and zoning codes to enhance infrastructure resilience and reduce the risks posed by soil liquefaction in earthquake-prone regions.

11. References

1. Galli, P., *New empirical relationships between magnitude and distance for liquefaction*. Tectonophysics, 2000. 324(3): p. 169-187. [https://doi.org/10.1016/S0040-1951\(00\)00118-9](https://doi.org/10.1016/S0040-1951(00)00118-9)
2. Kokusho, T., *Innovative earthquake soil dynamics*. 2017: CRC Press. <https://doi.org/10.1201/9781315645056>
3. Zhou, J., et al., *Feasibility of stochastic gradient boosting approach for evaluating seismic liquefaction potential based on SPT and CPT case histories*. Journal of Performance of Constructed Facilities, 2019. 33(3): p. 04019024. [https://doi.org/10.1061/\(ASCE\)CF.1943-5509.0001292](https://doi.org/10.1061/(ASCE)CF.1943-5509.0001292)
4. Khanbabazadeh, H., *Nonlinearity effect on the dynamic behavior of the clayey basin edge*. Geomechanics and Engineering, 2024. 36(4): p. 367-380. <https://doi.org/10.12989/gae.2024.36.4.367>.
5. Khanbabazadeh, H., R. Iyisan, and B. Ozaslan, Seismic behavior of the shallow clayey basins subjected to obliquely incident wave. Geomech. Eng, 2022. 31(2): p. 183-195. <https://doi.org/10.12989/gae.2022.31.2.183>
6. Khanbabazadeh, H., R. Iyisan, and B. Ozaslan, *2D seismic response of shallow sandy basins subjected to obliquely incident waves*. Soil Dynamics and Earthquake Engineering, 2022. 153: p.107080. <https://doi.org/10.1016/j.soildyn.2021.107080>
7. Matsuoka, M., et al., *Evaluation of liquefaction potential for large areas based on geomorphologic classification*. Earthquake Spectra, 2015. 31(4): p. 2375-2395. <https://doi.org/10.1193/072313EQS211M>
8. Bahrainy, H. and A. Bakhtiar, *Manjil Earthquake of June 20, 1990, The Lessons Learned, in Urban Design in Seismic-Prone Regions*. 2022, Springer International Publishing: Cham. p. 49-95. DOI: <https://doi.org/10.1007/978-3-031-08321-1>
9. Uyanik, O., *Soil liquefaction analysis based on soil and earthquake parameters*. Journal of Applied Geophysics, 2020. 176: p. 104004 <https://doi.org/10.1016/j.jappgeo.2020.104004>
10. Ahmad, M., et al., *Application of machine learning algorithms for the evaluation of seismic soil liquefaction potential*. Frontiers of Structural and Civil Engineering, 2021. 15(2): p. 490-505. <https://doi.org/10.1007/s11709-020-0669-5>
11. García, S., M. Romo, and E. Ovando- Shelley, *Machine learning for assessing liquefaction potential of soils*.
12. Liu, C. and J. Macedo, *Machine learning- based models for estimating liquefaction- induced building settlements*. Soil Dynamics and Earthquake Engineering, 2024. 182: p. 108673. <https://doi.org/10.1016/j.soildyn.2024.108673>
13. Abbasimaeleh, P., *Soil liquefaction in seismic events: pioneering predictive models using machine learning and advanced regression techniques*. Environmental Earth Sciences, 2024. 83(7): p. 189. <https://doi.org/10.1007/s12665-024-11480-x>
14. Ozsagir, M., et al., *Machine learning approaches for prediction of fine-grained soils liquefaction*. Computers and Geotechnics, 2022. 152: p. 105014. <https://doi.org/10.1016/j.compgeo.2022.105014>
15. Obaidullah ,S., *Preliminary Liquefaction Susceptibility Using Different Machine Learning Techniques*. 2024, (SCEE), NUST.
16. Kumar, D., et al., *A novel methodology to classify soil liquefaction using deep learning*. Geotechnical and Geological Engineering, 2021. 39 :p. 1049-1058 <https://doi.org/10.1007/s10706-020-01544-7>.
17. Raja, M.N.A., T. Abdoun, and W. El-Sekelly, *Smart prediction of liquefaction-induced lateral spreading*. Journal of Rock Mechanics and Geotechnical Engineering, 2024. 16(6): p. 2310-2325. <https://doi.org/10.1016/j.jrmge.2023.05.017>
18. Mohammadikish, S., et al., *Soil liquefaction assessment by CPT and VS data and incomplete-fuzzy C-means clustering*. Geotechnical and Geological Engineering, 2024. 42(3): p. 2205-2220. <https://doi.org/10.1007/s10706-023-02669-1>
19. Şehmusoğlu, E.H., T.F. Kurnaz, and C. Erden, *Estimation of soil liquefaction using artificial intelligence techniques: an extended comparison between machine and deep learning approaches*. Environmental Earth Sciences, 2025.84(5): p. 1-22. <https://doi.org/10.1007/s12665-025-12116-4>
20. Niu, F., et al., *Ultra-high performance concrete: A review of its material properties and usage in shield tunnel segment*. Case Studies in Construction Materials, 2025: p. e04194. <https://doi.org/10.1016/j.cscm.2024.e04194>
21. Agha Kasiri, Sh., Agha Kasiri, S., Ghazawi,M., Farrokhzad, F. *Investigation of Sandy Soil Settlement Due to Liquefaction Under Earthquake in PILE Group*. International Conference on Architecture, Urban Planning, Art, Industrial Design, Construction and Technology of Hikmat-e-Bonyan. 2025. <https://civilica.com/doc/2235759>
22. Agha Kasiri, Sh., Emami Korandeh, M., Mohammadi, Gh., Taban, A. *Deep Learning-Based Fluidity Data Evaluation*. International Conference on

Architecture, Urbanism, Art, Industrial Design, Construction and Technology Hekmat-Bonyan, 2025. <https://civilica.com/doc/2235758>

23. Agha Kasiri, Sh., Agha Kasiri, S., Farrokhzad, F., Qadawi, M. *Comparison of settlement in single pile and pile group under dynamic loading*. Fourth International Congress of Civil Engineering, Architecture and Urban Development, 2016. <https://civilica.com/doc/617967>

24. Agha Kasiri, Sh., Farrokhzad, F., Qadawi, M. *Determination of bearing capacity and settlement of piles in sandy soil in static and dynamic mode*. International Conference on New Horizons in Civil Engineering, Architecture and Urban Planning and Cultural Management of Cities, 2016. <https://civilica.com/doc/567742>

25. Marzouk, I., et al., *A case study on advanced CPT data interpretation: from stratification to soil parameters*. Geotechnical and Geological Engineering, 2024. 42(5): p. 4087-4113. <https://doi.org/10.1007/s10706-024-02774-9>

26. Seed, H.B. and I.M. Idriss, *Simplified procedure for evaluating soil liquefaction potential*. Journal of the Soil Mechanics and Foundations division, 1971. 97(9): p. 1249-1273. <https://doi.org/10.1061/JSFEAQ.0001662>

27. Liao, S.S. and R.V. Whitman, *Overburden correction factors for SPT in sand*. Journal of geotechnical engineering, 1986. 112(3): p. 373-377. [https://doi.org/10.1061/\(ASCE\)0733-9410\(1986\)112:3\(373\)](https://doi.org/10.1061/(ASCE)0733-9410(1986)112:3(373))

28. Robertson, P.K. and C. Wride, *Evaluating cyclic liquefaction potential using the cone penetration test*. Canadian geotechnical journal, 1998. 35(3): p. 442-459. <https://doi.org/10.1139/t98-017>

29. Robertson, P.K., *Soil classification using the cone penetration test*. Canadian geotechnical journal, 1990. 27(1): p. 151-158. <https://doi.org/10.1139/t90-014>

30. ÖNorm, E., *I [6Eurocode 7: Entwurf. Berechnung und Bemessung in der Geotechnik–Teil, 1997. 1.*

31. Robertson, P.K., *Interpretation of cone penetration tests—a unified approach*. Canadian geotechnical journal, 2009. 46(11): p. 1337-1355.

32. Robertson, P.K. *Soil behaviour type from the CPT: an update*. in *2nd International symposium on cone penetration testing*. 2010. Cone Penetration Testing Organizing Committee Huntington Beach.

33. Robertson, P.K., *Cone penetration test (CPT)-based soil behaviour type (SBT) classification system—an update*. Canadian Geotechnical Journal, 2016. 53(12): p. 1910-1927.

34. Robertson, P.K. and K. Cabal, *Guide to cone penetration testing for geotechnical engineering*. Signal Hill, CA: Gregg Drilling & Testing, 2015.

35. Niu, F., et al., *Ultra-high performance concrete: A review of its material properties and usage in shield tunnel segment*. Case Studies in Construction Materials, 2025: p. e04194.

36. Boulanger, R.W. and I.M. Idriss, *CPT and SPT based liquefaction triggering procedures*. Report No. UCD/CGM-14, 2014. 1: p. 134.

37. Shen, M., et al., *Predicting liquefaction probability based on shear wave velocity: an update*. Bulletin of Engineering Geology and the Environment, 2016. 75: p. 1199-1214. <https://doi.org/10.1007/s10064-016-0880-8>

38. Haykin, S., *Neural networks and learning machines*, 3/E. 2009: Pearson Education India

39. Ross, T.J., *Fuzzy logic with engineering applications*. 2005: John Wiley & Sons.